Magnetoelectric transitions of a distorted triangular-lattice antiferromagnet in a magnetic field

Tota Nakamura
College of Engineering, Shibaura Institute of Technology, Minuma-ku, Saitama 330-8570, Japan
(Received 6 March 2011; revised manuscript received 12 July 2011; published 9 August 2011)

Large-scale Monte Carlo simulations are performed to analyze magnetoelectric transitions of a spin-lattice model in a magnetic field. The model explains well an experimental field-temperature phase diagram of $RbCoBr_3$. The magnetic structure in each phase is determined. Simultaneous magnetoelectric transitions observed in the zero-field case are found to occur only in the low-field region, whereas magnetic transitions and electric transitions are decoupled in the high-field region. When the spin-lattice correlation is weak, an asymmetric ferrimagnetic state and a half-ferrimagnetic state appear. The former is the intermediate state between the partial-disordered state and the ferrimagnetic state. The latter phase is characterized by a sublattice order parameter with a $\frac{\uparrow}{2}$-$\frac{\uparrow}{2}$-$\downarrow$ ordering pattern.

DOI: 10.1103/PhysRevB.84.054429 PACS number(s): 75.80.+q, 75.40.Mg, 77.80.−e, 75.30.Kz

I. INTRODUCTION

Frustration is an important key word in recent developments of magnetic materials.[1] Ordinary magnetic order is destroyed by frustration and new exotic states may appear. The ground state of a frustrated system is usually unstable against small perturbations, and such magnetic systems sometimes couple to other degrees of freedom to relax frustration. The interplay between magnetism and electricity in so-called magnetoelectric (ME) multiferroic materials is a typical example and is heavily investigated nowadays.[2] A main concern of this paper is also the ME effect found in ABX_3-type antiferromagnets.

ABX_3-type antiferromagnets are typical frustrated magnets. Let us restrict our attention to Ising antiferromagnets, in which the magnetic ions are located on triangular-lattice planes, which are stacked in the c-axis direction. There have been many investigations both experimentally[3–7] and theoretically.[8–15] These compounds are characterized by spin frustration and a quasi-one-dimensionality. Frustration is caused by antiferromagnetic interactions on the triangular lattice. Exchange interactions along the c axis are larger than those on the triangular-lattice plane, so the correlation length along the c axis becomes very long.

In the absence of a magnetic field, successive magnetic phase transitions occur. The low-temperature magnetic structure is the ferrimagnetic state. There exists a partial-disordered (PD) phase between the paramagnetic phase and the ferrimagnetic phase. In the PD phase, one of three sublattices is completely disordered, while the other two sublattices take antiferromagnetic configurations.

The $KNiCl_3$ family of compounds are regarded as distorted triangular-lattice antiferromagnets.[16–18] They exhibit structural phase transitions as well as magnetic phase transitions. Because each BX_3 chain has a negative charge, these compounds have both magnetic and electric character. The magnetic phase transitions and the electric phase transitions usually occur at different temperatures.

Morishita and co-workers[19,20] found that the magnetic transition and the electric transition occur at the same temperature in $RbCoBr_3$. This simultaneous ME transition is a very rare finding in ABX_3 compounds. The real and imaginary parts of the dielectric constant show an anomaly at 37 K, where the magnetic phase transition is observed by neutron experiments.[21–23] These magnetic and electric measurements revealed that the phase transitions in $RbCoBr_3$ are quite unusual among the $KNiCl_3$ family of compounds. The electric transition temperature is 37 K, which is very low compared to that of other compounds. The transition usually takes place around room temperature. The magnetic PD phase appears in a much narrower temperature region. The growth of the ferrimagnetic order is very slow. These unusual characteristics are well understood by considering the frustrated spin-lattice model proposed by Shirahata and Nakamura.[24] Nishiwaki and Todoroki[25] discussed the appearance of the three-sublattice (asymmetric) ferrielectric state using the mean-field approximation. Nakamura and Nishiwaki[26] modified the spin-lattice model and explained the experimental results quantitatively by Monte Carlo (MC) simulations.

Recently, Nishiwaki *et al.*[27] reported a high-field magnetization experiment on this compound. They obtained a field-temperature (H-T) phase diagram from a small dM/dH anomaly in the magnetization process. As the applied magnetic field decreases, the transition temperatures approach two successive transition temperatures at zero field. The experimental results suggest that successive phase transitions occur even in a magnetic field. However, it is not yet accepted whether the small dM/dH anomaly observed in the experiment corresponds to the real phase transition. Motivated by the experimental results explained above, we perform MC simulations on the spin-lattice model in a uniform magnetic field. Our aim is to clarify whether or not successive ME transitions occur. We investigate the possibility of controlling the transitions with a magnetic field. Another aim is to determine the magnetic structure of each ordered phase. It is not yet known experimentally whether or not the PD state exists in a magnetic field.

The present paper is organized as follows. We explain our model Hamiltonian in Sec. II. Our numerical method is explained in Sec. III, and the results are presented in Sec. IV. A discussion is presented in Sec. V.

II. SPIN-LATTICE MODEL

We use the theoretical model proposed in a previous paper.[26] This is a phenomenological model that explains the

experimental results of $RbCoBr_3$. Our aim is to understand the ME effects of this compound as simply as possible. There is no microscopic derivation of the model, and we neglect long-range interactions of electric dipoles and quantum effects. The former are very important in electric systems and the latter are important at low temperatures. Therefore, this model partly succeeds in explaining the experiment quantitatively but partly fails owing to a lack of microscopic accountability to the real compound.

Let us briefly explain the model here. Consider a stacked triangular lattice with an Ising spin variable $S_{ij} = \pm 1/2$ and a lattice variable $\sigma_{ij} = \pm 1/2$ at each site. Here, the subscript i denotes the position in the c axis, and j denotes the position on the ab plane. We neglect the transverse spin components, S^x and S^y, for simplicity, although these may be important at low temperatures, where quantum fluctuations become relevant. The lattice variable σ_{ij} denotes the displacement from the symmetric lattice point along the c axis. Each ion is considered to shift either upward ($\sigma_{ij} = 1/2$) or downward ($\sigma_{ij} = -1/2$).

The Hamiltonian consists of the lattice part $\mathcal{H}_{\rm L}$ and the spin part $\mathcal{H}_{\rm S}$, written as $\mathcal{H} = \mathcal{H}_{\rm L} + \mathcal{H}_{\rm S}$, where

$$\mathcal{H}_{\rm L} = -2J_c^{\rm L}\sum_{i,j}\sigma_{ij}\sigma_{(i+1)j} - 2J_1^{\rm L}\sum_{i}\sum_{\langle jk\rangle}^{\rm n.n.}\sigma_{ij}\sigma_{ik} - 2J_2^{\rm L}\sum_{i}\sum_{\langle jk\rangle}^{\rm n.n.n.}\sigma_{ij}\sigma_{ik}, \tag{1}$$

$$\mathcal{H}_{\rm S} = -2J_c^{\rm S}\sum_{i,j}S_{ij}S_{(i+1)j} - 2J_1^{\rm S}\sum_{i}\sum_{\langle jk\rangle}^{\rm n.n.}(1-\Delta(\sigma_{ij}-\sigma_{ik})^2)S_{ij}S_{ik} - 2J_2^{\rm S}\sum_{i}\sum_{\langle jk\rangle}^{\rm n.n.n.}(1-\Delta(\sigma_{ij}-\sigma_{ik})^2)S_{ij}S_{ik} - g\mu_B H\sum_{i,j}S_{i,j}. \tag{2}$$

Here, H denotes a uniform magnetic field. Each subscript (c, 1, 2) denotes a direction of the interaction: c denoting along the c axis, 1 denoting nearest-neighbor (nn) pairs on the ab plane, and 2 denoting next-nearest-neighbor (nnn) pairs on the ab plane. The lattice part is a realization of the elastic energy, $(\sigma_{ij} - \sigma_{i'j'})^2$, and $J^{\rm L}_{(c,1,2)}$ is the spring constant.

The nn spin-spin interaction is antiferromagnetic ($J_1^{\rm S} < 0$) and the nnn interaction is ferromagnetic ($J_2^{\rm S} > 0$) to realize the ferrimagnetic ground state. Interactions along the c axis are antiferromagnetic ($J_c^{\rm S} < 0$), and the magnitudes are set as $|J_c^{\rm S}| \gg |J_1^{\rm S}|, |J_2^{\rm S}|$ because of the quasi-one-dimensionality. Spins along the c-axis order antiferromagnetically first. The uniform magnetization vanishes in the ground state. When we apply a uniform magnetic field to this system, a local magnetization is induced in a region where the antiferromagnetic order is broken. The sign of $J_c^{\rm L}$ is positive (ferroelectric) and those of $J_1^{\rm L}$ and $J_2^{\rm L}$ are set negative (antiferroelectric). Therefore, there is frustration in the lattice system as in the spin system. Assumptions of the lattice system are consistent with exclusion volume effects.

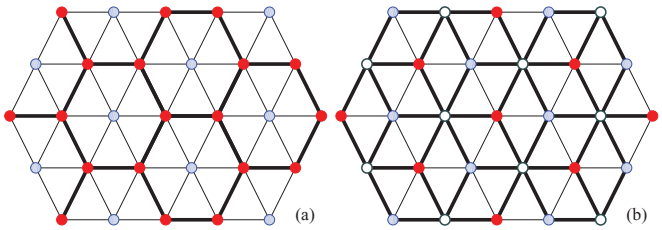

FIG. 1. (Color online) Relaxation of frustration by the lattice distortion. Filled red circles depict c chains shifting upward. Filled blue circles depict c chains shifting downward. Open circles depict c chains not shifting. Thin (thick) lines depict weak (strong) magnetic interactions. (a) When the lattice is deformed to a lattice-ferri (↑-↑-↓) configuration, the spin-PD state is favored. (b) When the lattice is deformed to a lattice-PD (↑-↓-0) configuration, the spin-ferri state is favored.

We suppose that the spin-spin exchange interactions depend on the lattice variables in this model. The magnetic interaction becomes weak if the exchange path is distorted. A parameter Δ is defined as the ratio of the distortion effect. When lattice distortion occurs, the magnetic interaction is reduced by $(1 - \Delta)$. The lattice system influences the spin system only by this term. Therefore, it serves as a spin-lattice coupling. We use the same value of Δ for $J_1^{\rm S}$ and $J_2^{\rm S}$ for simplicity. The exchange path along the c axis is rigid against ion shift and hence we assume $J_c^{\rm S}$ to be unaffected.

The spin-lattice coupling produces the following stable ordering patterns as discussed earlier by Plumer *et al.*[28] for static lattice distortion. When the lattice takes a ↑-↑-↓ configuration, the PD state of the spin system is favored, as shown in Fig. 1(a). We call the lattice ↑-↑-↓ configuration "lattice ferri," and the PD state of the spin system "spin PD," in this paper. In contrast, when the lattice system takes a ↑-↓-0 configuration, the ferrimagnetic spin state is favored, as shown in Fig. 1(b). We call the lattice ↑-↑-0 configuration "lattice PD," and the ferrimagnetic state of the spin system "spin ferri," in this paper.

III. MONTE CARLO METHOD

Spin states and lattice states are updated separately and alternatively in the present simulations. When a spin state or a lattice state is updated, the molecular fields from the interacting spin and lattice states are calculated. We apply both the axial-cluster-flip algorithm[29,30] and the single-spin-flip algorithm. When all the spin states and the lattice states are updated, we count one MC step. Our cluster-flip algorithm solves for the slowdown that is caused by the long correlation length along the c axis. Therefore, the MC step needed to equilibrate the system depends little on the temperature or the magnetic field except in the very vicinity of the transition temperature.

An axial-cluster-flip algorithm[29,30] is an application of the cluster-flip algorithm[31–36] of the quantum MC method. The c axis in our model is regarded as the Trotter axis in the quantum MC method. A distinct difference from the original cluster-flip algorithms is that a cluster is only defined along one c axis at one spin site on the ab plane. We do not connect spins on the ab plane.

The present cluster algorithm works well when no magnetic field is applied.[26] However, we have to modify the algorithm and use the single-spin-flip algorithm together at the same time in simulations with a magnetic field. The nn magnetic interactions along the c axis, J_c, are antiferromagnetic in our model. We transform them to ferromagnetic ones by rotating every other spin direction by 180°. A uniform magnetic field becomes a staggered magnetic field after this transformation. In this situation, whether a cluster length is an even or an odd number is important. When it is even, the magnetic field term in the Hamiltonian vanishes. This term only remains when the cluster length is an odd number. Therefore, we cannot make the c axis continuous as in the original cluster-flip algorithm; it must remain an integer. To determine a discrete cluster length, we first generate an exponential random number as in the continuous imaginary-time cluster-flip algorithm.[32,36] The mean value of a random number is the correlation length along the c axis, ξ_c. Then we convert the random number to an integer and set it to a cluster length. Since the one-dimensional Ising spin model is solved exactly, we use an exact expression for ξ_c written as

$$\xi_c^{-1} = \ln\left(\frac{\left(\cosh(\beta H)+\sqrt{\sinh^2(\beta H)+\exp[4\beta J_c^S]}\right)^2}{\exp[4\beta J_c^S]-1}\right), \tag{3}$$

where β is the inverse temperature. It is noted from this expression that the correlation length does not depend on the direction of the magnetic field. If we apply this cluster flip alone, spin states with field $+H$ and spin states with field $-H$ are mixed. The net magnetization always becomes 0 in this case. Therefore, a single-spin-flip algorithm is also applied after the cluster flip to select spin states that are relevant to the direction of the magnetic field. A mixture of spin states with different magnetic directions accelerates the MC dynamics with the fields.[37]

We observe in the present MC simulations the following physical quantities: the sublattice order parameters, 1/3-structure factors, 1-structure factors, and the uniform magnetic susceptibility. The sublattice order parameters for the lattice part, m_η^L, and the spin part, m_η^S, are defined as

$$m_\eta^L = \frac{1}{N_{\rm sub}}\sum_i\sum_{j\in\eta}\sigma_{ij}, \tag{4}$$

$$m_\eta^S = \frac{1}{N_{\rm sub}}\sum_i(-1)^i\sum_{j\in\eta}S_{ij}, \tag{5}$$

where $\eta = 1,2,3$ denote one of three sublattices in the triangular lattice, and $N_{\rm sub} \equiv N/3$. Note that we need the $(-1)^i$ phase factor owing to the antiferromagnetic order along the c axis. The structure factors are defined by the sublattice order parameters as

$$\left(f_{1/3}^L\right)^2 = \frac{1}{8}\left\langle\sum_{\eta=1,2,3}\left(m_\eta^L - m_{\eta+1}^L\right)^2\right\rangle, \tag{6}$$

$$\left(f_{1/3}^S\right)^2 = \frac{1}{8}\left\langle\sum_{\eta=1,2,3}\left(m_\eta^S - m_{\eta+1}^S\right)^2\right\rangle, \tag{7}$$

$$\left(f_1^L\right)^2 = \left\langle\left(m_1^L + m_2^L + m_3^L\right)^2\right\rangle, \tag{8}$$

$$\left(f_1^S\right)^2 = \left\langle\left(m_1^S + m_2^S + m_3^S\right)^2\right\rangle. \tag{9}$$

Detailed simulation procedures are the same as in our previous paper.[26] We use the mixed phase initialization,[38–40] where we prepare several initial spin-lattice states and spatially mix them. It is a standard initialization method when a first-order transition occurs. A typical number of initialization MC steps is 10 000. The total number of MC steps is set to more than 30 000 near the transition temperature. We performed mostly from 10 to 50 independent MC runs and took the average over these runs. The linear size of the system on the ab plane is $L = 59$, and that along the c axis, L_c, is a multiple of 4 that is closest to $59\xi_c$. The total number of spins is roughly $59^3\xi_c$, and there are on average 59^3 correlated clusters in this system. As a typical example in the H-T phase diagram, when $H = 15$ T and $T = 25$ K, the correlation length is $\xi_c = 27.6$ and the c-direction lattice size is $L_c = 1632$. The total spin number is 5.8 million in this case. It exceeds 38 million at the lowest temperature at which the simulation is performed. We may consider the system size to be sufficiently large. Our aim is not to accurately calculate the phase transition temperatures but to compare them to the experimental data and to determine the magnetic structures. Therefore, it is sufficient to use the raw simulation data in our analyses without any finite-size scaling.

The physical parameters in our spin-lattice Hamiltonian were estimated in our previous paper[26] as $J_c^S = -97$ K, $J_1^S = -2.4$ K, $J_2^S = 0.14$ K, $J_c^L = 73$ K, $J_1^L = -49$ K, $J_2^L = 0.38$ K, and $\Delta = 0.20$. However, a mean-field-like approximation was applied in that simulation. For an update of a spin (lattice) state, the interacting lattice (spin) states were replaced with a mean value along the c axis. This approximation might influence the numerical estimates of physical parameters and the phase transition properties. We do not apply this approximation in the present simulations. Therefore, we first check the physical parameters by comparing the numerical results to the experimental results when the magnetic field is not applied. The results are shown in Fig. 2, which presents the neutron experimental data and the magnetic susceptibility data. The MC data reproduce the experimental results very well. The parameters are determined as

$$\begin{aligned} &J_c^S = -95\text{ K}, \quad J_1^S = -3.0\text{ K}, \quad J_2^S = 0.13\text{ K},\\ &J_c^L = 74\text{ K}, \quad J_1^L = -50\text{ K}, \quad J_2^L = 0.21\text{ K},\\ &\Delta = 0.20. \end{aligned} \tag{10}$$

These parameters are consistent with the previous estimates. We use the parameters of Eq. (10) in all simulations in this paper.

IV. RESULTS

A. Successive phase transitions in the low-field region

In this section we examine successive phase transitions and spin-lattice ordering patterns when the magnetic field is weak. Particularly, we focus on the issue of whether or not a small magnetic field affects the ordering patterns and the phase transitions. When a magnetic field is not applied, there are five

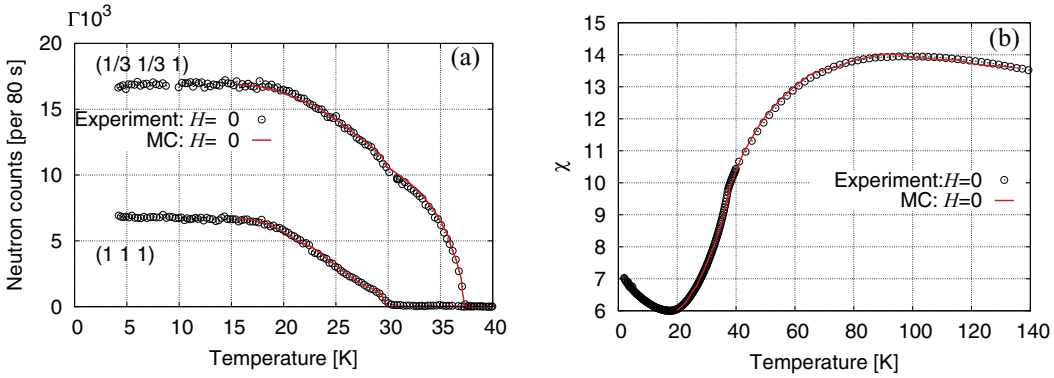

FIG. 2. (Color online) (a) MC data on the structure factor compared with neutron experimental data.[23] MC data are multiplied to coincide with experimental data. (b) MC data on the uniform magnetic susceptibility compared with experimental data.[22] Amplitudes of the simulation data and a constant contribution from the nonmagnetic impurity are determined so that the maximum value and the minimum value agree with the experimental data.

different spin-lattice ordering patterns, which are divided by two spin transitions and two lattice transitions.[26] We apply a 5-T magnetic field and observe the sublattice order parameters. The result is compared to the zero-field result, as shown in Fig. 3. Let us first explain the zero-field case.

The first magnetic transition occurs at 37 K, which is usually referred to as T_{N1}. The sublattice order parameters jump to small finite values. Then they continuously increase as the temperature decreases. As shown in Fig. 3(c), no algebraic relaxation is observed in the nonequilibrium process of our MC simulations. Relaxation functions on the high-temperature side exhibit exponential decays and those on the low-temperature side exhibit convergences, indicating a first-order transition.[41]

The second transition, at 36 K, is a simultaneous, first-order spin-lattice transition. Spin and lattice systems are strongly correlated and assist each other in changing their states.

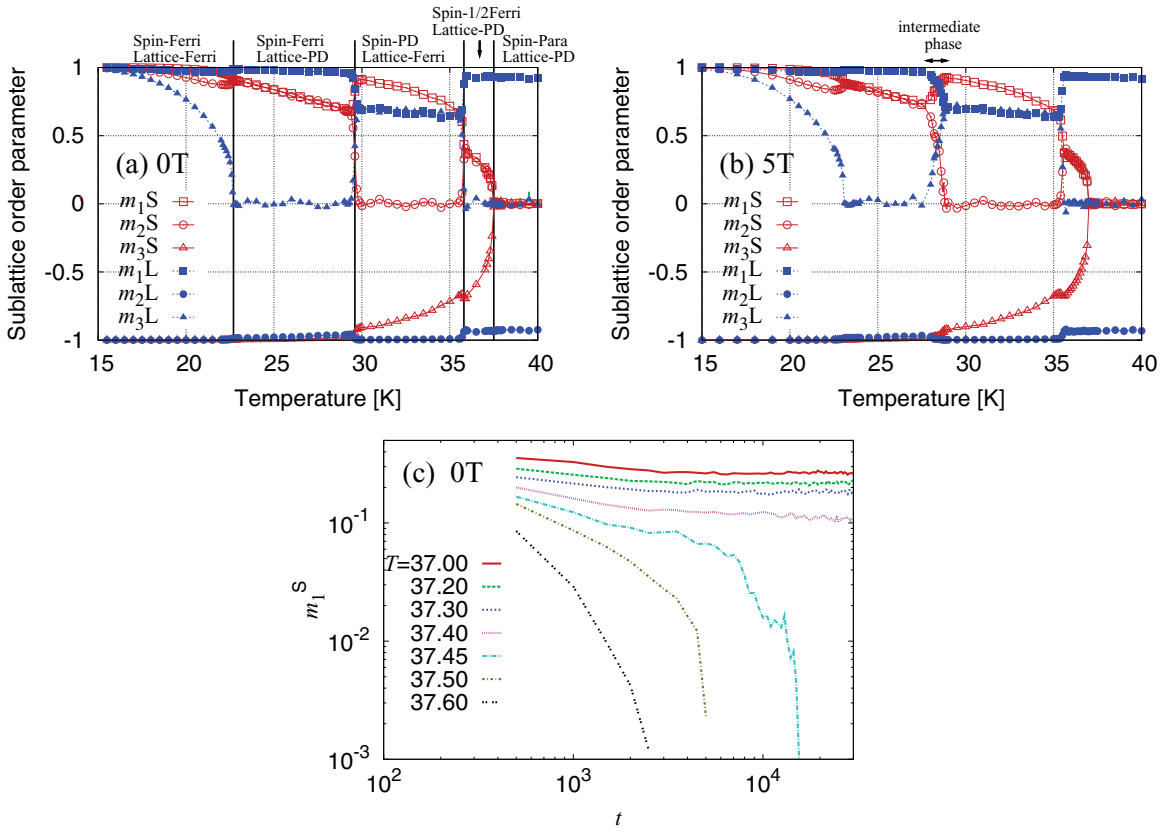

FIG. 3. (Color online) Sublattice profiles of spin variables and lattice variables. (a) Zero-field case: $H = 0$ T. (b) Small-field case: $H = 5$ T. The amplitude is normalized to unity when the sublattice order is perfect. Data for each sublattice, 1, 2, and 3, are plotted with squares, circles, and triangles, respectively. Spin-lattice ordering patterns are denoted in the upper margin of (a). (c) Relaxation functions of the sublattice order parameter, m_1^{S}, near the first transition temperature, $T_{\mathrm{N1}} = 37$ K when $H = 0$ T.

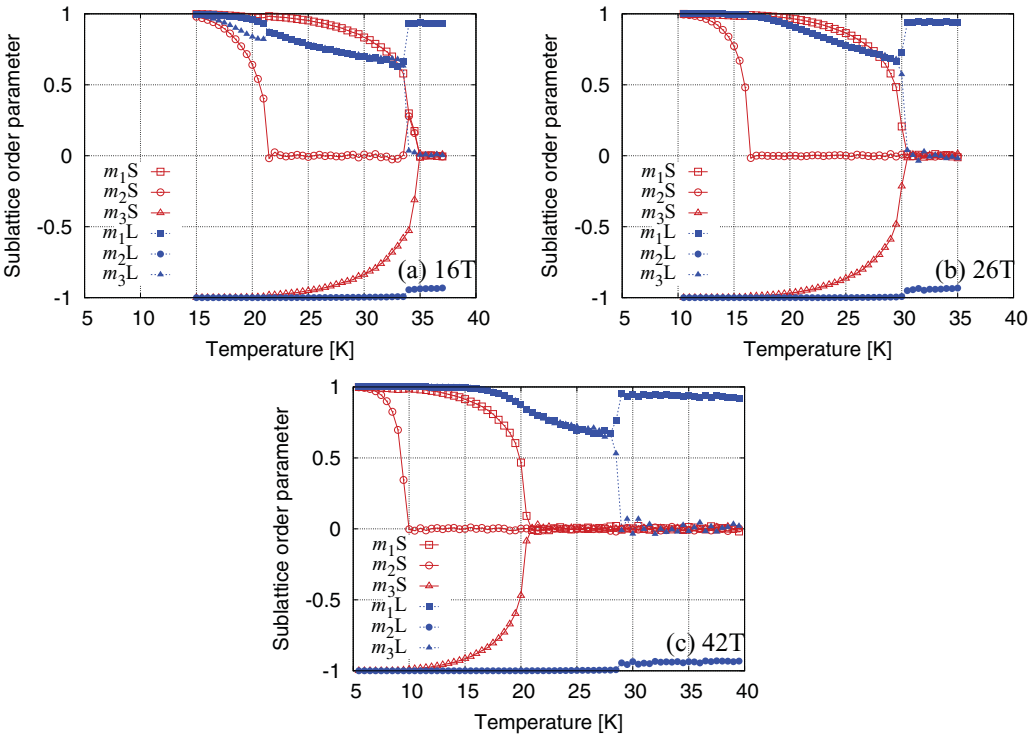

FIG. 4. (Color online) Sublattice profiles of spin-lattice variables for applied magnetic fields of (a) $H = 16$ T, (b) $H = 26$ T, and (c) $H = 42$ T. The amplitude is normalized to unity when the sublattice order is perfect. Data for each sublattice are plotted with squares, circles, and triangles, respectively.

The ground state of the lattice system appears below this temperature. Therefore, the transition is mainly driven by the lattice degrees of freedom. The spin-PD state appears because it is favored by both spin-lattice coupling and the entropy effects of the spin system.

The third transition, at 29.6 K, is usually referred to as T_{N2}. It is also a simultaneous, first-order spin-lattice transition. This transition is mainly driven by the spin degrees of freedom because the ground state of the spin system (spin-ferri state) is realized on the low-temperature side. The lattice system gives up to take its ground-state configuration.

The fourth transition, at 23 K, is driven by the lattice degrees of freedom. The lattice system takes an asymmetric ferrielectric state in the low-temperature region. The space group changes from $P\bar{3}c1$ to $P3c1$. An asymmetric ferrimagnetic state also appears in the spin system. These asymmetric spin-lattice states recover symmetry as the temperature decreases. The ground state of the whole spin-lattice system is realized below 15 K, and it is a perfect ferrimagnetic and ferrielectric state.

A new finding in the zero-field case is the appearance of a "half-ferrimagnetic state" below T_{N1}. Magnitudes of the up-spin states are one-half the magnitudes of the down-spin states, as represented by $\frac{\uparrow}{2}$-$\frac{\uparrow}{2}$-$\downarrow$. The summation of the three sublattice order parameters vanishes, an outcome of the spin-lattice coupling. The spin-PD ($\uparrow$-0-$\downarrow$) state usually appears below this transition temperature, because it is favored by entropy effects of the spin system. In contrast, the lattice system [lattice-PD($\uparrow$-$\downarrow$-0) state] favors the spin-ferri ($\uparrow$-$\uparrow$-$\downarrow$) state through the spin-lattice coupling energy. The half-ferrimagnetic state appears as a compromise between these two states. Since the summation of the spin sublattice order parameters vanishes, the neutron experiment alone cannot distinguish the half-ferrimagnetic state from the PD state. Another experiment that can detect the inner molecular field is needed.

When a magnetic field is applied, temperature dependencies of the order parameters mostly agree with those of the zero-field case, with the exception of the third phase transition. The transition temperature shifts to the low-temperature side, and an intermediate ordering pattern appears. The order parameters continuously change in this phase. Since the third transition is mainly driven by the spin degrees of freedom, the magnetic field is relevant to changing the nature of the phase transition, effectively weakening the spin-lattice correlation.

B. *H*-*T* phase diagram

We examine temperature dependencies of the sublattice order parameters up to a high-field region and determine the spin-lattice transition temperatures. Typical examples are shown in Fig. 4. As the magnetic field increases, the spin-lattice correlation becomes weaker. The spin transition and the lattice transition occur independently in the high-field region.

We summarize the results and plot a phase diagram in Fig. 5. The g value is set to 5.2 to fit the MC phase boundary to the experimental results. The simulation results of the spin-driven transition temperatures are consistent with the experimental results. This consistency continues until the temperature reaches 20 K. Clearly the small $\mathrm{d}M/\mathrm{d}H$ anomaly observed in the magnetization process experiment

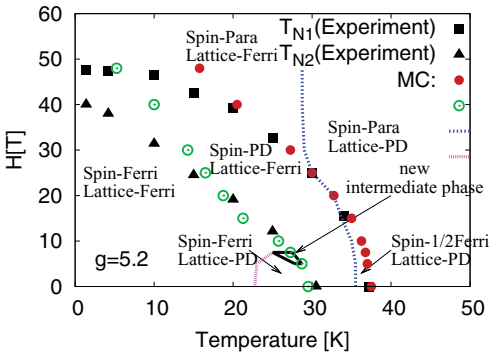

FIG. 5. (Color online) An H-T phase diagram of the present spin-lattice model compared with the experimental results on $RbCoBr_3$.[27] Circles depict spin-driven transition points, and lines depict lattice-driven transition points. A spin-lattice ordering pattern in each phase is also denoted.

signals the magnetic phase transition, a conclusion also verified by the fact that the spin-driven transition temperature strongly depends on the field. However, the lattice-driven transition temperatures are rather robust, depending on the magnetic field only when the simultaneous spin-lattice transition occurs in the low-field region.

We compare the MC results with the experimental results in the phase diagram (Fig. 5). At lower temperatures, the spin-PD state is stabilized in a wider region in the real compound. The present theoretical model is only valid when the temperature is higher than 20 K. We have neglected the S^x and S^y components of the magnetic spins. These quantum fluctuations may destabilize the ferrimagnetic state and stabilize the spin-PD state. Dielectric measurements[22] have also revealed that another structural transition occurs at 9 K. The real compound at low temperatures may be beyond the valid range of our model.

The spin-PD phase and the half-ferrimagnetic phase clearly exist in a magnetic field. The half-ferrimagnetic state becomes unstable in the high-field region. It disappears when $H \geqslant 20$ T. This is the magnetic field at which the first spin-driven transition temperature [filled (red) circles in Fig. 5] coincide with the lattice-driven transition temperature [dotted (blue) line in Fig. 5]. Both transitions occur simultaneously in the field range of $20 \leqslant H < 30$ T.

C. Magnetization process and the structure factor

Let us consider other physical observables in the magnetic field in this section. First, we compare our magnetization process results with the experimental results[27] as shown in Fig. 6. Figure 6(a) shows the raw magnetization data, and Fig. 6(b) shows the numerical differentials. An impurity effect (Van Vleck term) is estimated from the slope in the low-field region. The plotted MC results include this term. The g value is set as $g = 5.2$, which is the same as estimated when we draw the phase diagram. Consistency between the experimental data and the MC data is excellent for the data at 34 and 20 K. The present model can explain the experimental results when $T \geqslant 20$ K. We can observe a small anomaly of dM/dH in the MC data, which is consistent with the experimental one. An experimental phase boundary between the paramagnetic phase and the PD phase (T_{N1}) can be determined by this anomaly. Nishiwaki *et al.*[27] also reported that a phase boundary between the PD phase and the ferrimagnetic phase can be determined by a small shoulder-like anomaly of dM/dH. However, we cannot observe such a small anomaly within our magnetic field resolution. Consistency between MC results and experimental results becomes poor at $T = 10$ K, and the raw magnetization data and the numerical differentiation do not agree with each other. The discrepancy is already exhibited at the phase boundary in Fig. 5. The spin-PD state is stabilized in a wider range in real $RbCoBr_3$ experiments. The discrepancy suggests that the theoretical model needs an additional fluctuation term to explain the low-temperature behavior.

Figure 7(a) shows the temperature dependence of the structure factors in a magnetic field. This is a theoretical prediction for the neutron experiments. The low-field data ($H = 5$ T) are consistent with the zero-field results. There are two characteristic behaviors in the low-field (and also the zero-field) data: one is a small jump of $f_{(1,1,1)}$ near 30 K, and the other is a slow increase in $f_{(1,1,1)}$ below 30 K that is almost linear with temperature. The small jump is caused by a sharp first-order transition from the spin-PD state to the symmetric spin-ferri state. The lattice system also changes state from the lattice-ferri state to the lattice-PD state. This sharp first-order transition occurs because a strong spin-lattice correlation assists in promoting a sudden and simultaneous configuration change. These characteristic behaviors disappear in the high-field region, where the spin

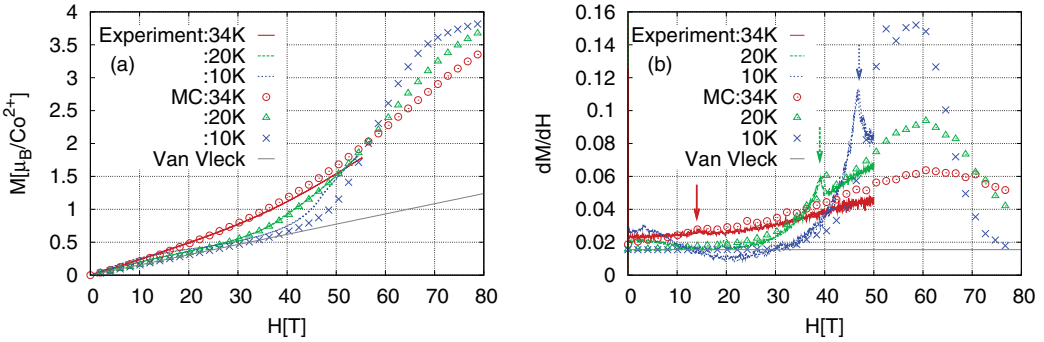

FIG. 6. (Color online) (a) Experimental results of the magnetization process compared with the MC results. The Van Vleck term is estimated from the slope in the low-field limit. The g value is set to 5.2. (b) Numerical differentiations of the magnetization data, dM/dH, plotted against the magnetic field. Arrows indicate the experimental phase boundary between the paramagnetic phase and the PD phase.

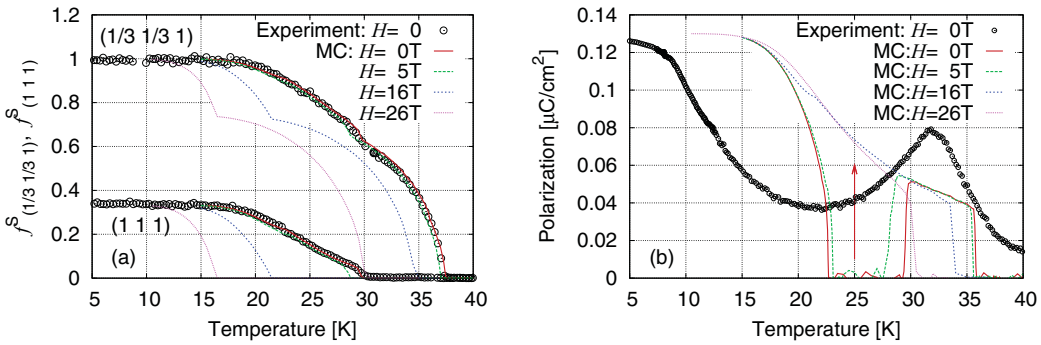

FIG. 7. (Color online) (a) Magnetic structure factor data and (b) electric polarization data in a magnetic field compared with zero-field experimental data. MC data are scaled so that the saturation values coincide with experimental data. The arrow depicts an increase in the polarization by the magnetic field.

and the lattice are decoupled. The first-order transition is weak in this situation. The asymmetric ferrimagnetic state becomes the low-temperature state as shown in Fig. 4. Only the 0 sublattice of the PD (↑-↓-0) state changes the state from disorder to a small order. As the temperature decreases, this order grows continuously and saturates to the full order. Therefore, the jump behavior disappears and the structure factor shows an upward bending (nonlinear) behavior with temperature. The temperature dependencies of the structure factors in the high-field region resemble those of $CsCoCl_3$, where the lattice system does not couple with the spin system.

Figure 7(b) shows the MC results of the spontaneous polarization compared with the experimental results.[22] The experimental data in the zero field exhibit a maximum at 32 K and a minimum at 23 K. A decrease in the polarization below $T = 32$ K is an unusual behavior, because the ground state is the polarized state. This re-entrant behavior corresponds to the low-field MC results, which exhibit a sudden vanishing at $T = 30$ K and a sudden appearance at $T = 23$ K. Although the quantitative consistency is poor, we may speculate from our MC results that the decreasing polarization below $T = 32$ K can be explained by the simultaneous spin-lattice transition from the lattice-ferri state to the lattice-PD state. The increasing polarization below 23 K can be explained by the spin-lattice transition from the lattice-PD state to the lattice-ferri state.

The present model is too simple for the lattice degrees of freedom. The experimental polarization data are partly contributed by Rb ions that are not taken into account in our model. However, the most characteristic temperature dependence of the polarization is observed in our simulations. If we consider that the present model can represent the most essential part of the lattice system in $RbCoBr_3$, we can also speculate that the polarization can be enhanced by applying a magnetic field in the intermediate temperature region, $20 \leqslant T \leqslant 30$. The arrow in Fig. 7(b) depicts this enhancement. When the magnetic field is larger than 16 T, the decrease in polarization disappears. The magnetic field decouples the spin system from the lattice system. The electric polarization, which has been suppressed by the spin-ferri order, is now free to take a finite order, leading to a positive ME correlation. An experimental check for this speculation is strongly desired.

V. DISCUSSION

The successive phase transitions of the spin-lattice system under a magnetic field are studied in connection to the experimental results on $RbCoBr_3$. When the magnetic field is weak, there are four successive transitions at low temperatures. The first spin transition [filled (red) circles in Fig. 5] occurs singly; it is not accompanied by a lattice transition. The other three transitions are simultaneous spin-lattice transitions. Only the spin-driven transition temperature [open (green) circles in Fig. 5] strongly depends on the magnetic field. The lattice-driven transition temperature is robust against the field. We may speculate that in the real ME system the transition may be driven by the electric degrees of freedom if the magnetic phase boundary does not depend on the magnetic field. As the magnetic field increases, the spin-lattice correlation becomes weaker. Both systems are finally decoupled in the high-field region. The magnetic field lowers only the spin-driven transition temperature. If the spin transition occurs at very low temperatures, the lattice order is already rigid. There is no room to change the lattice state cooperatively with the spin system. This is the scenario for spin-lattice decoupling by a magnetic field.

All phase transitions discussed in the phase diagram are first-order phase transitions. No algebraic relaxation is observed in the nonequilibrium process of the MC simulations, as shown in Fig. 3(c). Since the spin system and the lattice system are connected by the spin-lattice coupling Δ, we must consider this spin-lattice system as one system with six sublattices. Even when the spin system is disordered, the lattice system has a finite order. This state is regarded as the PD state in the whole spin-lattice system. The first magnetic transition [filled (red) circles in Fig. 5] is the first-order transition of this type. Note that this transition is the second-order one if there is no spin-lattice coupling. A small spin-lattice coupling makes the first-order phase transition. The change in the sublattice order parameter is not sharp, with the order continuously growing as the temperature decreases. An asymmetric ferrielectric or ferrimagnetic state appears at low temperatures. Although the existence of the asymmetric ferrimagnetic state was predicted by the mean-field theory,[8,25] whether this state is just an artifact of the theory has not been clarified. The present simulations make it clear that the asymmetric state exists and continuously

changes to the symmetric state without any phase transition. The temperature dependence of the $f_{(1,1,1)}$ structure factor shows an upward bending in this case, consistent with the experimental results of $CsCoCl_3$, which is a typical ABX_3 Ising antiferromagnet. Therefore, we may speculate that the low-temperature magnetic ordered state in real compounds is the asymmetric ferrimagnetic state. It becomes the symmetric ferrimagnetic state when the $f_{(1,1,1)}$ structure factor saturates at low temperature.

In the low-field region we found a half-ferrimagnetic state, which is the product of a compromise between the spin-PD state and the spin-ferri state. The half value of the sublattice order parameter is uniformly distributed within the ab plane; it is not a summation of the spin-PD cluster and the spin-ferri cluster separated by the domain wall. The half-ferrimagnetic state has not been predicted in the spin-only system and it appears with the help of the lattice system. This state may be a sign of spin-lattice coupling. Experiments that can detect the internal field distribution, such as μ-SR, are expected to check this theoretical prediction.

ACKNOWLEDGMENTS

The author would like to thank Dr. Y. Nishiwaki for provision of the experimental data and for fruitful discussions. This work was supported by Grant-in-Aid for Scientific Research No. 21540343 from the Ministry of Education, Culture, Sports, Science and Technology, Japan.

[1]For example, see articles in *Proceedings of the International Conference on Highly Frustrated Magnetism, Osaka, Japan*, 15–19 August 2006 [J. Phys. Condens. Matter **19**, 14 (2007)].
[2]For a review, see T. Arima, J. Phys. Soc. Jpn. **80**, 052001 (2011).
[3]W. B. Yelon, D. E. Cox, and M. Eibschütz, Phys. Rev. B **12**, 5007 (1975).
[4]M. Mekata and K. Adachi, J. Phys. Soc. Jpn. **44**, 806 (1978).
[5]M. F. Collins and O. A. Petrenko, Can. J. Phys. **75**, 605 (1997).
[6]M. Mao, B. D. Gaulin, R. B. Rogge, and Z. Tun, Phys. Rev. B **66**, 184432 (2002).
[7]H. Kuroe, A. Oosawa, T. Sekine, Y. Nishiwaki, and T. Kato, J. Phys. Soc. Jpn. **76**, 043713 (2007).
[8]H. Shiba, Prog. Theor. Phys. **64**, 466 (1980).
[9]F. Matsubara and S. Inawashiro, J. Phys. Soc. Jpn. **53**, 4373 (1984).
[10]O. Heinonen and R. G. Petschek, Phys. Rev. B **40**, 9052 (1989).
[11]T. Kurata and H. Kawamura, J. Phys. Soc. Jpn. **64**, 232 (1995).
[12]M. L. Plumer and A. Mailhot, Physica A **222**, 437 (1995).
[13]O. Koseki and F. Matsubara, J. Phys. Soc. Jpn. **69**, 1202 (2000).
[14]N. Todoroki and S. Miyashita, J. Phys. Soc. Jpn. **73**, 412 (2004).
[15]E. Meloche and M. L. Plumer, Phys. Rev. B **76**, 174430 (2007).
[16]D. Visser, G. C. Verschoor, and D. J. W. Ijdo, Acta Crystallogr. Sec. B **36**, 28 (1980).
[17]K. Adachi, K. Takeda, F. Matsubara, M. Mekata, and T. Haseda, J. Phys. Soc. Jpn. **52**, 2202 (1983).
[18]T. Mitsui, K. Michida, T. Kato, and K. Iio, J. Phys. Soc. Jpn. **63**, 839 (1994).
[19]K. Morishita, T. Kato, K. Iio, T. Mitsui, M. Nasui, T. Tojo, and T. Atake, Ferroelectrics **238**, 105 (2000).
[20]K. Morishita, K. Iio, T. Mitsui, and T. Kato, J. Magn. Magn. Mater. **226–230**, 579 (2001).
[21]Y. Nishiwaki, T. Kato, Y. Oohara, and K. Iio, J. Phys. Soc. Jpn. **73**, 2841 (2004).
[22]Y. Nishiwaki, H. Imamura, T. Mitsui, H. Tanaka, and K. Iio, J. Phys. Soc. Jpn. **75**, 094702 (2006).
[23]Y. Nishiwaki, A. Oosawa, T. Nakamura, K. Kakurai, N. Todoroki, N. Igawa, Y. Ishii, and T. Kato, J. Phys. Soc. Jpn. **77**, 104703 (2008).
[24]T. Shirahata and T. Nakamura, J. Phys. Soc. Jpn. **73**, 254 (2004).
[25]Y. Nishiwaki and N. Todoroki, J. Phys. Soc. Jpn. **75**, 024708 (2006).
[26]T. Nakamura and Y. Nishiwaki, Phys. Rev. B **78**, 104422 (2008).
[27]Y. Nishiwaki, M. Tokunaga, T. Nakamura, N. Todoroki, and T. Kato, J. Phys. Soc. Jpn. **79**, 084707 (2010).
[28]M. L. Plumer, A. Caillé, and H. Kawamura, Phys. Rev. B **44**, 4461 (1991).
[29]T. Nakamura, Phys. Rev. Lett. **101**, 210602 (2008).
[30]T. Nakamura and Y. Ito, J. Phys. Soc. Jpn. **72**, 2405 (2003).
[31]H. G. Evertz, G. Lana, and M. Marcu, Phys. Rev. Lett. **70**, 875 (1993).
[32]B. B. Beard and U.-J. Wiese, Phys. Rev. Lett. **77**, 5130 (1996).
[33]R. Rieger and N. Kawashima, Eur. Phys. J. B **9**, 233 (1999).
[34]H. W. J Blöte and Y. Deng, Phys. Rev. E **66**, 066110 (2002).
[35]S. V. Isakov and R. Moessner, Phys. Rev. B **68**, 104409 (2003).
[36]H. G. Evertz, Adv. Phys. **52**, 1 (2003).
[37]O. Redner, J. Machta, and L. F. Chayes, Phys. Rev. E **58**, 2749 (1998).
[38]C. Rebbi, Phys. Rev. D **21**, 3350 (1980).
[39]F. Fucito and A. Vulpiani, Phys. Lett. A **89**, 33 (1982).
[40]Y. Ozeki, K. Kasono, N. Ito, and S. Miyashita, Physica A **321**, 271 (2003).
[41]Y. Ozeki and N. Ito, J. Phys. A **40**, R149 (2007).